Quantifying non-Newtonian effects in the context of transitional rotating boundary layers

P. T. Griffiths[1]*

ISROMAC 2016

International Symposium on Transport Phenomena and Dynamics of Rotating Machinery

Hawaii, Honolulu

April 10-15, 2016

Abstract

The stability of the boundary-layer on a rotating disk is considered for fluids that adhere to a non-Newtonian governing viscosity relationship. For fluids with shear-rate dependent viscosity the base flow is no longer an exact solution of the Navier-Stokes equations, however, in the limit of large Reynolds number the flow inside the three-dimensional boundary-layer can be determined via a similarity solution.

The convective instabilities associated with flows of this nature are described both asymptotically and numerically via separate linear stability analyses. Akin to previous Newtonian studies it is found that there exists two primary modes of instability; the upper-branch type I modes, and the lower-branch type II modes. Results show that both these modes can be stabilised or destabilised depending on the choice of non-Newtonian viscosity model. A number of comments are made regarding the suitability of some of the more well-known non-Newtonian constitutive relationships within the context of the rotating disk model. Such a study is presented with a view to suggesting potential control mechanisms for flows that are practically relevant to the turbo-machinery industry.

Keywords

Rotating boundary layers — Non-Newtonian — Convective instability

[1] *Department of Engineering, University of Leicester, Leicester, United Kingdom*

*__Corresponding author__: paul.griffiths@le.ac.uk

1. INTRODUCTION

The stability and transition of the boundary-layer on a rotating disk is a classical fluid mechanics problem that has attracted a great deal of attention from numerous authors over many decades. In the Newtonian limit there exists a vast wealth of material concerning the solutions of the rotating disk equations.

The pioneering study of Gregory *et al.* [1] contains the first observation of the stationary cross-flow vortices on a rotating disk. The flow is convectively unstable, within certain regions, to disturbances stationary in the frame rotating with the disk. These disturbances are excited by roughnesses on the surface and, because these roughnesses are fixed in time in the rotating frame, the stationary disturbances are consistently excited and reinforced such that they are evident in flow-visualisation experiments.

Theoretical studies of convective modes within the rotating-disk system have shown that the flow is susceptible to two distinct modes of instability. The type I (upper-branch) mode due to the cross-flow instability and the type II (lower-branch) mode attributed to external streamline curvature. Because of this the neutral curve has a characteristic two-lobed structure, as noted by Malik [2] and Lingwood [3], amongst others. Hall [4] demonstrated that in the limit of large Reynolds number the upper and lower branches of the neutral curve can be described (with excellent agreement) using an asymptotic theory. More recently, the aforementioned pioneering studies have been extended to include rotating spheres, see Garrett & Peake [5] and rotating cones, see Garrett *et al.* [6]. In both cases the flow can be stabilised (or destabilised) with control of the governing parameter, that being the angle of latitude, in the case of the sphere, and the half-angle, in the case of the cone. Indeed, research on the von Kármán boundary-layer remains a topic of active study, the interested reader is referred to the recent review article by Lingwood & Alfredsson [7].

Rotating disk flows have practical relevance to turbo-machinery where non-Newtonian fluids are commonplace. However, far less attention has been given to the corresponding non-Newtonian rotating disk problem. Very recently Griffiths [8] determined the base flow profiles for numerous generalised Newtonian fluid models. Using these results we investigate the convective instability of the boundary-layer on a rotating disk for shear-thinning power-law and Carreau fluids. Results show that accurately modelling the variation of viscosity within the boundary-layer is of paramount importance.

2. FORMULATION

We consider the flow of a steady incompressible non-Newtonian fluid due to an infinite rotating plane located at $z^* = 0$ (here the superscript * denotes dimensional quantities). The plane rotates about the z^*-axis with angular velocity Ω^*. The motion of the fluid is in the positive z^* direction, the fluid is infinite in extent and the only boundary is located at $z^* = 0$. In a rotating frame of reference the continuity and Navier-Stokes equations are expressed as

$$\boldsymbol{\nabla}^* \cdot \boldsymbol{u}^* = 0, \tag{1a}$$

$$\frac{\partial \boldsymbol{u}^*}{\partial t^*} + \boldsymbol{u}^* \cdot \boldsymbol{\nabla}^* \boldsymbol{u}^* + \boldsymbol{\Omega}^* \times (\boldsymbol{\Omega}^* \times \boldsymbol{r}^*) + 2\boldsymbol{\Omega}^* \times \boldsymbol{u}^* = -\frac{1}{\rho^*}\boldsymbol{\nabla}^* p^* + \frac{1}{\rho^*}\boldsymbol{\nabla}^* \cdot \boldsymbol{\tau}^*. \quad (1b)$$

Here $\boldsymbol{u}^* = (\tilde{U}^*, \tilde{V}^*, \tilde{W}^*)$ are the velocity components in cylindrical polar coordinates (r^*, θ, z^*), t^* is time, $\boldsymbol{\Omega}^* = (0, 0, \Omega^*)$ and $\boldsymbol{r}^* = (r^*, 0, z^*)$. The fluid density is ρ^* and p^* is the fluid pressure. For generalised Newtonian models, such as the power-law model, the stress tensor is given by $\boldsymbol{\tau}^* = \mu^*(\dot{\gamma}^*)\dot{\boldsymbol{\gamma}}^*$, where $\dot{\boldsymbol{\gamma}}^* = \boldsymbol{\nabla}^* \boldsymbol{u}^* + (\boldsymbol{\nabla}^* \boldsymbol{u}^*)^{\mathrm{T}}$ is the rate of strain tensor and $\mu^*(\dot{\gamma}^*)$ is the non-Newtonian viscosity. The magnitude of the rate of strain tensor is $\dot{\gamma}^* = \sqrt{(\dot{\boldsymbol{\gamma}}^* : \dot{\boldsymbol{\gamma}}^*)/2}$. The governing relationships for $\mu^*(\dot{\gamma}^*)$ that will be considered herein are:

$$\mu^* = m^*(\dot{\gamma}^*)^{n-1}, \quad (2a)$$

$$\mu^* = \mu^*_\infty + (\mu^*_0 - \mu^*_\infty)[1 + (\lambda^*\dot{\gamma}^*)^2]^{(n-1)/2}, \quad (2b)$$

these are the power-law and Carreau models, respectively. Here m^* is the consistency coefficient and n is the fluid index, for $n > 1$ the fluid is said to be shear-thickening, whilst for $n < 1$ the fluid is said to be shear-thinning. The Newtonian viscosity relationship is recovered when $n = 1$ and $\mu^*_0 = \mu^*_\infty$, respectively. The infinite-shear-rate viscosity is μ^*_∞, the zero-shear-rate viscosity is μ^*_0 and λ^* is the characteristic time constant, often referred to as the 'relaxation time'.

In the Newtonian limit an exact solution of (1) exists, as was first determined by von Kármán [9]. However, no such solution exists for flows with $n \neq 1$. It is only in the large Reynolds number limit that the leading order boundary-layer equations admit a similarity solution analogous to the exact Newtonian solution. The governing boundary-layer equations are given in Griffiths [8], for brevity we exclude these here.

We introduce the generalisation of the classic Newtonian similarity solution in order to solve for the steady mean flow relative to the disk. The dimensionless similarity variables are defined by

$$U(\eta) = \frac{\tilde{U}^*_0}{r^*\Omega^*}, \quad V(\eta) = \frac{\tilde{V}^*_0}{r^*\Omega^*}, \quad W(\eta) = \frac{\tilde{W}^*_0}{\chi^*}, \quad P(\eta) = \frac{\tilde{P}^*_1}{\rho^*(\chi^*)^2}, \quad (3)$$

where $\chi^* = [\nu^*/(r^{*^{1-q}}\Omega^{*^{1-2q}})]^{1/(q+1)}$. Here $(\tilde{U}^*_0, \tilde{V}^*_0, \tilde{W}^*_0)$ are the leading order velocity components, $\tilde{P}^*_1$ is the leading order fluid pressure term and $\nu^* = \sigma^*/\rho^*$ is the kinematic viscosity. The dimensionless similarity coordinate is $\eta = r^{(1-q)/(q+1)}z$, where here r and z have been made dimensionless with respect to $L^* = (\nu^*/\Omega^{*^{2-q}})^{1/2}$. For power-law fluids $q = n$ and $\sigma^* = m^*$, whereas for Carreau fluids $q = 1$ and $\sigma^* = \mu^*_\infty$.

Thus the laminar-flow profiles are determined from the following set of non-linear ordinary differential equations:

$$2U + \bar{\eta}U' + W' = 0, \quad (4a)$$

$$U^2 - (V+1)^2 + (W + \bar{\eta}U)U' - (\mu U')' = 0, \quad (4b)$$

$$2U(V+1) + (W + \bar{\eta}U)V' - (\mu V')' = 0, \quad (4c)$$

where $\bar{\eta} = \eta(1-q)/(q+1)$ and the primes denote differentiation with respect to η. The power-law viscosity function is given by

$$\mu = (U'^2 + V'^2)^{(n-1)/2}, \quad (4d)$$

whilst the Carreau viscosity function takes the form

$$\mu = 1 + c_0[1 + k^2(U'^2 + V'^2)]^{(n-1)/2}. \quad (4e)$$

Here $c_0 = (\sigma^* - \mu^*_0)/\sigma^*$ is the viscosity ratio, and $k = r^*\lambda^*\Omega^*(\rho^*\Omega^*/\sigma^*)^{1/2}$ is the dimensionless equivalent of λ^*. Throughout this study we fix the values of c_0 and k such that $c_0 = 1$ and $k = 100$, this is consistent with previous investigations.

Using a fourth-order Runge-Kutta quadrature routine twinned with a Newton iteration scheme to determine the values of the unknowns $U'(0)$ and $V'(0)$ the set of ordinary differential equations are solved subject to

$$U(0) = V(0) = W(0) = 0, \quad U(\eta \to \infty) \to 0, \quad V(\eta \to \infty) \to -1. \quad (5)$$

Although the formulation here is different these results are an exact reproduction of those presented by Griffiths [8]. The laminar-flow profiles are presented in figures 1 (power-law) and 2 (Carreau) for a range of shear-thinning values of n.

The differences between the base flow profiles, and their significance in relation to the resulting linear stability calculations, will be discussed in section 4.

3. STABILITY ANALYSES

3.1 Type I asymptotic analysis

This analysis is based on the assumption that the Reynolds number is large and that the disturbances have wavelengths scaled on the boundary-layer thickness, given by $\delta = Re^{-1/(q+1)}$. Here Re is the asymptotic representation of the Reynolds number. When considering the type I modes we observe the existence of three distinct layers. An inviscid layer, or zone, a wall layer and a critical layer. The inviscid zone encompasses the entirety of the boundary-layer, the wall layer is needed to ensure the no-slip condition at the wall is satisfied and the critical layer exists so that the singularities that arise within the inviscid zone are smoothed out.

By solving for zero-order perturbations in the linear disturbance equations we arrive at a modified form of Rayleigh's equation that is dependent on the parameter n. At the next order we determine a nonhomogeneous modified form of Rayleigh's equation that is required to match our leading order solution in the wall layer. This wall layer solution is given in terms of the decaying Airy function. Despite the appearance of additional viscous terms in the leading order governing equations we find that analytic solutions are obtainable. Matching these solutions between the two layers enables us to plot solutions for the asymptotic wavenumber and wave angle of the disturbances as functions of $R = r^{2/(q+1)}Re^{1/(q+1)}$. Here R is the numerical representation of the Reynolds number. Doing so enables us to make direct comparisons between the asymptotic and numerical solutions.

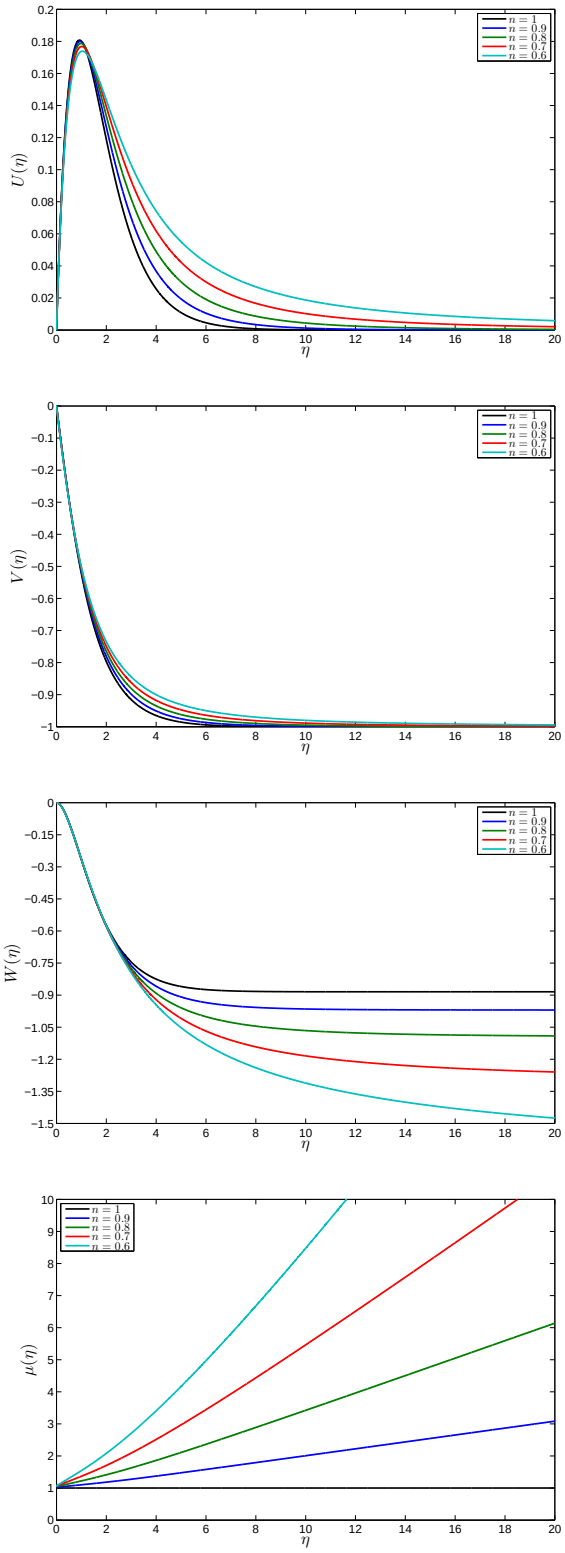

Figure 1. Plots of U, V, W and μ versus η for power-law fluids with $n = 1, 0.9, 0.8, 0.7, 0.6$. The η-axis has been truncated at $\eta = 20$.

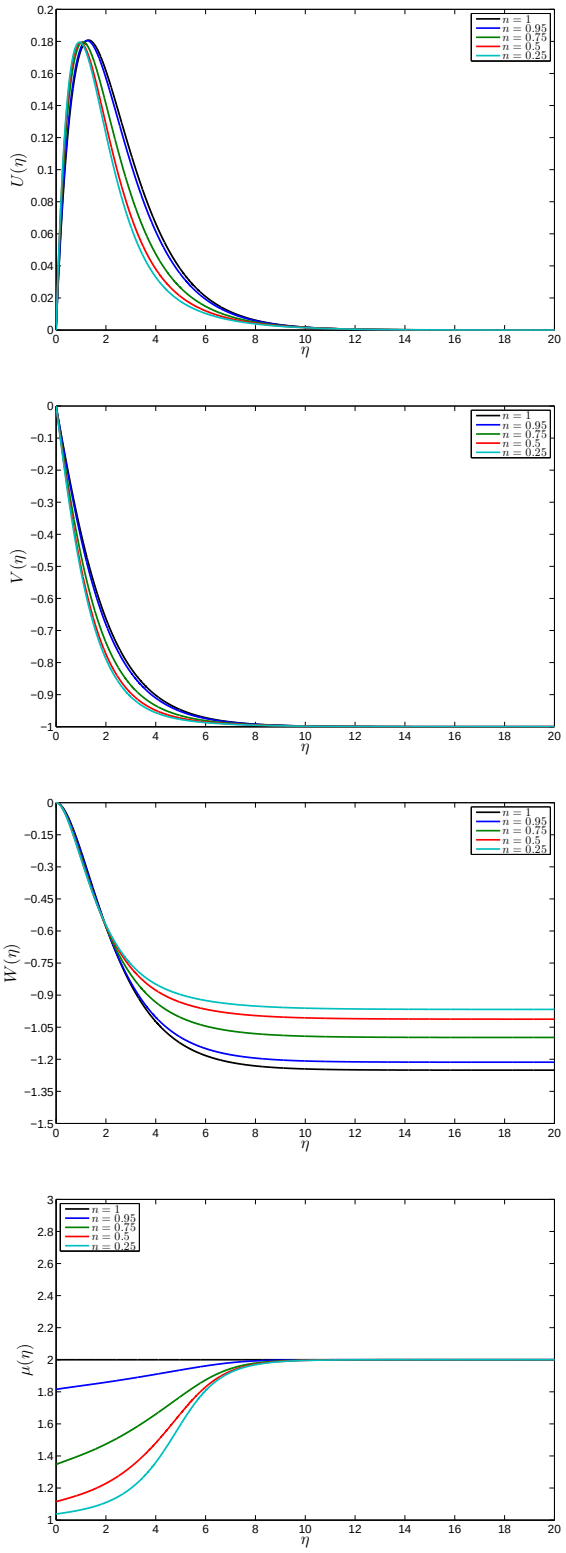

Figure 2. Plots of U, V, W and μ versus η for Carreau fluids with $n = 1, 0.95, 0.75, 0.5, 0.25$. The η-axis has been truncated at $\eta = 20$.

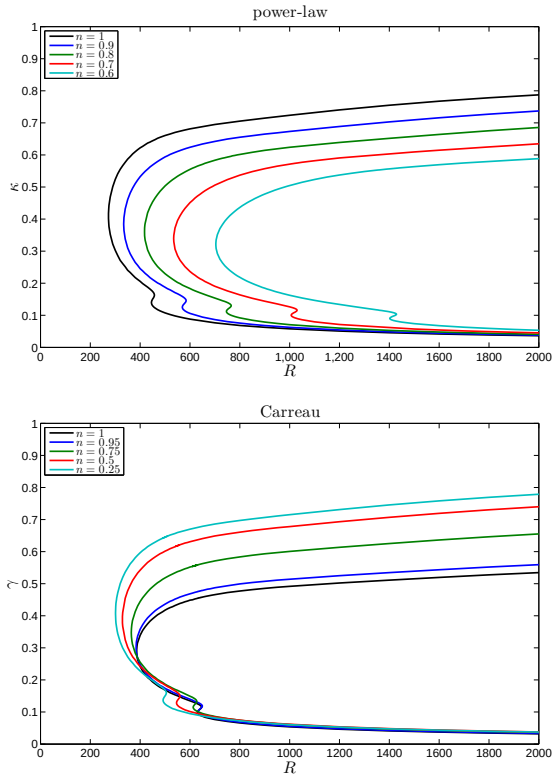

Figure 3. Wavennumber neutral stability curves for shear-thinning power-law fluids and Carreau fluids.

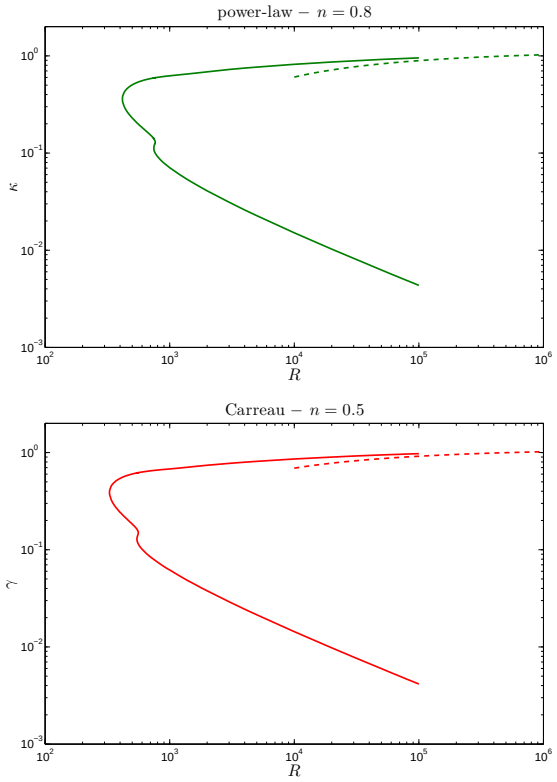

Figure 4. Neutral stability curves for large R with corresponding asymptotic predictions. Excellent agreement is observed in both cases for every n in the range of interest.

In this study we present only the type I asymptotic analysis with the viewpoint of validating our numerical results when the Reynolds number is large. Indeed initial investigations have begun on the corresponding type II analysis, we hope to report on this investigation in due course. For more details regarding the type I analysis see Griffiths *et al.* [10].

3.2 Numerical analysis

The stability analysis, applied at a specific radius, involves imposing infinitesimally small disturbances on the steady mean flow, in the form of scaled normal-mode quantities

$$(u, v, w, p) = (\hat{u}, \hat{v}, \hat{w}, \hat{p})(\eta; \alpha, \beta, \omega; R, n)e^{\mathrm{i}(\alpha r + \beta\theta - \omega t)}. \quad (6)$$

The frequency of the disturbance in the rotating frame is ω (taken to be zero in this stationary study), the complex radial wavenumber is $\alpha = \alpha_r + \alpha_i$ and β is the real azimuthal wavenumber.

After making an approximation akin to the parallel-flow assumption and a viscous assumption stemming from the asymptotic results, the stability equations may be written as sets of six first-order ODEs using transformed perturbing variables $\phi_i(\eta)$ with $i = 1, 2 \ldots 6$. The governing power-law equations can be found in Griffiths *et al.* [11], the equivalent Carreau fluid equations can be easily inferred from there. In all that follows the eigenvalue problem defined by the stability equations is solved with the homogeneous boundary conditions

$$\phi_i = 0 \quad \text{at} \quad \eta = 0, \quad (7a)$$
$$\phi_i \to 0 \quad \text{as} \quad \eta \to \infty, \quad (7b)$$

for all i. This eigenvalue problem is solved for certain combinations of values of α, β and ω at each Reynolds number, R, and for the specified value of n. From these we form the dispersion relation, $D(\alpha, \beta, \omega; R, n) = 0$, at each n, with the aim of studying the convective instabilities. The step size in η was reduced and the value of infinity increased until there were no discernible differences in the numerical results. The values taken were such that the boundary layer was approximated by 2000 equally spaced data points between $\eta = 0$ and $\eta = 20$. This discretization is known to be consistent with Lingwood [3] and Garrett & Peake [12], for example, and represents an appropriate balance between accuracy and computational effort for each n.

In order to investigate the structure of the spatial branches at each n, we solve the dispersion relation for α whilst marching through values of β at fixed R. For each n in the particular range of interest two spatial branches determine the convective instability characteristics of the system. Neutral curves, defined by $\alpha_i = 0$, have been calculated for a variety of shear-thinning values of n using both the power-law and Carreau fluid models.

4. DISCUSSION & CONCLUSIONS

Our results, both asymptotic and numerical, predict differing behaviour for shear-thinning fluids described by the power-law model when compared to those described by the Carreau model. We observe from figure 3 that the power-law model predicts a strong stabilising effect as the fluid index is decreased, whereas the Carreau model suggests that shear-thinning destabilises the boundary-layer flow. Under the power-law regime the value of the critical Reynolds number significantly decreases with n, as does the area encompassed by the neutral curves. Contrary to this, using the Carreau fluid model, we predict that the critical Reynolds number will be marginally increased as the shear-thinning parameter is increased, and moreover the area encompassed by the neutral curve will also significantly increase.

Figure 4 outlines the excellent agreement obtained between the results of the asymptotic analysis when compared to our numerical solutions. The large Reynolds number asymptotic analysis does indeed predict boundary-layer stabilisation in the power-law limit and destabilisation in the Carreau limit. This is wholly consistent with the numerical predictions at much lower Reynolds numbers.

The opposing results for our two shear-thinning models are indeed quite striking. These surprising results are attributed to the inability of the power-law model to describe shear-thinning flows for vanishing shear-rates, i.e. far from the disk surface. It is well known that for shear-thinning power-law fluids $\mu^*(\dot{\gamma}^* \to 0) \to \infty$, which is exemplified by our base flow solutions where we see that the viscosity function grows without bound as we move away from the surface of the disk, or equivalently move towards a region of low shear-rate. This essentially has the effect of increasing the predicted boundary-layer thickness. Contrastingly, we have that $\mu^*(\dot{\gamma}^* \to 0) \to \mu_0^*$ for shear-thinning Carreau fluids. Thus, far from the disk, in regions of low shear-rate, we find that $\mu \to 1 + c_0$, and in this case the boundary-layer thickness is reduced. It is this failing of the power-law model in regions of low shear rates that dramatically affects the predicted velocity profiles and therefore our linear stability results.

It transpires that the inability of the power-law model to accurately describe shear-thinning flows in the limit as $\dot{\gamma}^* \to 0$ has such a significant effect on the base flow profiles that it in turn effects the predicted stability characteristics. Therefore it is with relative confidence that we can say that the results owing from the Carreau model do indeed provide a much better description of the observed cross-flow instabilities.

These results clearly show the importance of accurately modelling the variation of viscosity within the boundary-layer. The power-law model may be useful for describing experimental results in regions of moderate shear-rate, however, it fails within this theoretical framework. As such, we conclude that the Carreau model provides a better physical representation of the boundary-layer flow and hence that the introduction of shear-thinning fluids will have a destabilising effect.

This work clearly motivates the need for detailed experimental results with which to compare our theoretical analysis. To the best of the author's knowledge no such experiments have yet taken place. Certainly in the Newtonian regime a wealth of literature exists, and this is currently a topic of particular interest, see Imayama *et al.* [13–15], for example. Personal communication with these authors has revealed the difficulty of obtaining consistently accurate experimental results; therefore we can only envisage the introduction of non-Newtonian fluids would serve to significantly complicate any experimental procedure.

It is acknowledged that the parallel-flow approximation utilised within the numerical stability analysis means that the perturbation equations solved here are not rigorous at $O(R^{-1})$. Although it is clear that the approximation will lead to inaccuracies at the predicted critical Reynolds numbers, it is our opinion that these will be small. The excellent agreement obtained between our numerical neutral curves and our asymptotic predictions shows that the effects of this approximation are negligible at high Reynolds number.

ACKNOWLEDGMENTS

The author gratefully acknowledges support from the Engineering and Physical Sciences Research Council UK.

REFERENCES

[1] N. Gregory, J. T. Stuart, and W. S. Walker. On the stability of three-dimensional boundary layers with applications to the flow due to a rotating disk. *Phil. Trans. R. Soc. Lond. A*, 248:155–199, 1955.

[2] M. R. Malik. The neutral curve for stationary disturbances in rotating-disk flow. *J. Fluid Mech.*, 164:275–287, 1986.

[3] R. J. Lingwood. Absolute instability of the boundary layer on a rotating disk. *J. Fluid Mech.*, 299:17–33, 1995.

[4] P. Hall. An asymptotic investigation of the stationary modes of instability of the boundary layer on a rotating disc. *Proc. R. Soc. Lond. A*, 406:93–106, 1986.

[5] S. J. Garrett and N. Peake. The stability and transition of the boundary layer on a rotating sphere. *J. Fluid Mech.*, 456:199–218, 2002.

[6] S. J. Garrett, Z. Hussain, and S. O. Stephen. The cross-flow instability of the boundary layer on a rotating cone. *J. Fluid Mech.*, 422:209–232, 2009.

[7] R. J. Lingwood and P. H. Alfredsson. Instabilities of the von Kármán Boundary Layer. *Appl. Mech. Rev.*, 67(3):030803, 2015.

[8] P. T. Griffiths. Flow of a generalised newtonian fluid due to a rotating disk. *J. Non-Newtonian Fluid Mech.*, 221:9–17, 2015.

[9] T. von Kármán. Über laminare und turbulente Reibung. *Z. Angew. Math. Mech.*, 1:233–252, 1921.

[10] P. T. Griffiths, S. O. Stephen, A. P. Bassom, and S. J. Garrett. Stability of the boundary layer on a rotating disk for power law fluids. *J. Non-Newtonian Fluid Mech.*, 207:1–6, 2014.

[11] P. T. Griffiths, S. J. Garrett, and S. O. Stephen. The neutral curve for stationary disturbances in rotating disk flow for power-law fluids. *J. Non-Newtonian Fluid Mech.*, 213:73–81, 2014.

[12] S. J. Garrett and N. Peake. The stability of the boundary layer on a rotating sphere in a uniform axial flow. *Euro. J. Mech.* B, 23:241–253, 2004.

[13] S. Imayama, P. H. Alfredsson, and R. J. Lingwood. A new way to describe the transition characteristics of a rotating-disk boundary-layer flow. *Phys. Fluids*, 24:031701, 2012.

[14] S. Imayama, P. H. Alfredsson, and R. J. Lingwood. An experimental study of edge effect on rotating-disk transition. *J. Fluid Mech.*, 716:638–657, 2013.

[15] S. Imayama, P. H. Alfredsson, and R. J. Lingwood. On the laminar-turbulent transition of the rotating-disk flow: the role of absolute instability. *J. Fluid Mech.*, 745:132–163, 2014.